ACS APPLIED MATERIALS & INTERFACES

Research Article

www.acsami.org

Transparent, Flexible Strain Sensor Based on a Solution-Processed Carbon Nanotube Network

Jieun Lee,[†] Meehyun Lim,[‡] Jinsu Yoon,[†] Min Seong Kim,[§] Bongsik Choi,[†] Dong Myong Kim,[†] Dae Hwan Kim,[†] Inkyu Park,*[,§] and Sung-Jin Choi*[,†]

[†]School of Electrical Engineering, Kookmin University, Seoul 02707, Korea

[‡]Mechatronics R&D Center, Samsung Electronics, Suwon, Gyeonggi-do 18448, Korea

[§]Department of Mechanical Engineering, KAIST, Daejeon 34141, Korea

Supporting Information

ABSTRACT: The demands for transparent, flexible electronic devices are continuously increasing due to their potential applications to the human body. In particular, skin-like, transparent, flexible strain sensors have been developed to realize multifunctional human−machine interfaces. Here, we report a sandwich-like structured strain sensor with excellent optical transparency based on highly purified, solution-processed, 99% metallic CNT−polydimethylsiloxane (PDMS) composite thin films. Our CNT−PDMS composite strain sensors are mechanically compliant, physically robust, and easily fabricated. The fabricated strain sensors exhibit a high optical transparency of over 92% in the visible range with acceptable sensing performances in terms of sensitivity, hysteresis, linearity, and drift. We also found that the sensitivity and linearity of the strain sensors can be controlled by the number of CNT sprays; hence, our sensor can be applied and controlled based on the need of individual applications. Finally, we investigated the detections of human activities and emotions by mounting our transparent strain sensor on various spots of human skins.

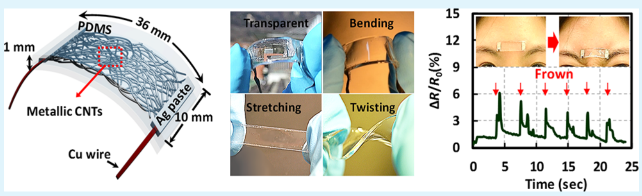

KEYWORDS: *carbon nanotube, strain sensor, transparent, polydimethylsiloxane (PDMS), solution-processed, network, sandwich-like structure*

INTRODUCTION

Strain sensors respond to mechanical deformations via a change in electrical signals such as capacitance or resistance. Many fundamental properties are required to fabricate high-performance strain sensors with high sensitivity and stretchability, fast response, excellent stability, low fabrication cost, and simplicity; however, conventional strain sensors composed of metal foils and semiconductors generally exhibit poor stretchability and sensitivity due to the brittle sensing materials.[1−5] In addition, these types of sensors are generally opaque; hence, the development of skin-like sensors[6] that stretch reversibly, that integrate with collapsible, stretchable, and mechanically robust displays[7] and solar cells,[8] and that can wrap around nonplanar and biological[9−11] surfaces, such as skin[12] and organs,[13] without wrinkling, are limited. Therefore, as alternatives to conventional strain sensors, many high-performance strain sensors have been actively developed by using nanomaterials and/or nanocomposites for high stretchability, sensitivity, and stability.[1,5,14−18] Recently, silver nanowires (AgNW) have actively been used as candidate material for future transparent, flexible electronics, particularly for high-performance strain sensors with great electrical and mechanical properties.[1,19] However, it has remained difficult to achieve high optical transparency with satisfactory electrical characteristics in AgNW-based strain sensors due to the high haze,[20] which results in low transmittance,[21] and the poor adhesion to flexible substrates.[20,22]

Carbon nanotubes (CNTs) have been widely used in flexible electronic devices, sensors, actuators, and biomaterials due to their excellent mechanical, electrical, and thermal properties.[15,18,23−26] Numerous types of strain sensors based on a percolated network of CNTs coupled with elastomer polymers,[18,27−29] such as polydimethylsiloxane (PDMS), have been intensively explored.[15,25,30,31] During the past several decades, in the field of CNT-based electronic devices, the difficulty in achieving high-purity carbon nanotubes (CNTs) during synthesis has led to extensive efforts in solution-processed purification, which has allowed CNTs to be rapidly and inexpensively separated based on their electronic types, such as semiconducting and metallic CNTs.[32−34] In particular, by using solution-processed CNTs, electronic devices with high breaking performances have been demonstrated by many research groups, including our own.[35−39] Hence, to combine excellent transparency and flexibility in strain sensors, highly purified, solution-processed metallic CNTs would be a good choice for use in high-performance strain sensors to achieve both high electrical performances and optical transparency.

Received: March 5, 2017
Accepted: July 13, 2017
Published: July 13, 2017

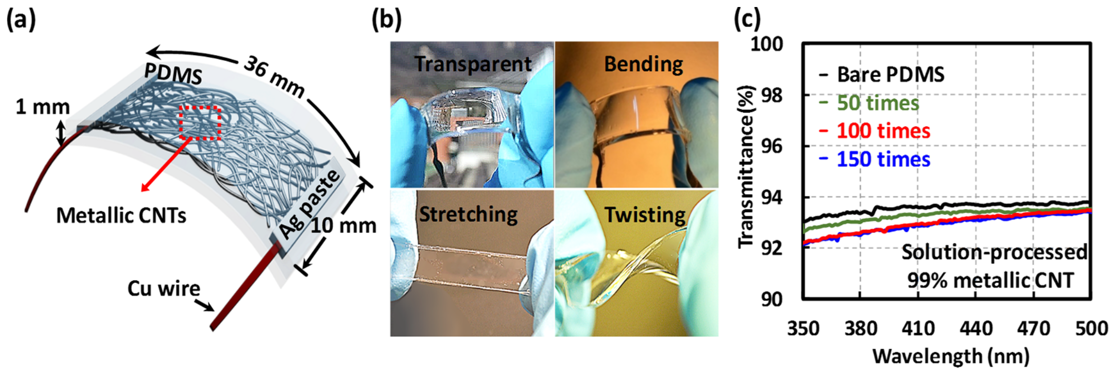

Figure 1. (a) Schematic illustration of the transparent CNT−PDMS composite strain sensor in the form of a sandwich structure (i.e., a solution-processed metallic CNT percolated network embedded between two layers of PDMS). (b) Image of the fabricated transparent CNT−PDMS strain sensor when it was bent, stretched, and twisted. (c) Optical transparency of the CNT−PDMS strain sensors with different number of sprays (50, 100, and 150 times) in the visible range. Bare PDMS film was also measured as a control sample.

This can be achieved by using a transparent percolated network of solution-processed metallic CNTs produced from a density-gradient ultracentrifugation (DGU) process[40] because the poorly conducting, strongly absorbing carbonaceous impurities and semiconducting CNTs can be eliminated to enhance optical transparency.[40,41]

In this paper, we demonstrate a transparent strain sensor based on composites of solution-processed metallic 99% CNTs and PDMS, i.e., metallic CNTs act as fillers and PDMS is used as a flexible substrate. We produced highly conductive, transparent, and stretchable CNT films with a high optical transparency of over 92% in visible ranges using a simple spray-coating method directly onto a PDMS substrate. There have been numerous reports on CNT−PDMS composite strain sensors;[15,25,30,31] however, to the best of our knowledge, no study has used highly purified, solution-processed metallic CNTs in a strain sensor with high transparency. Using our CNT−PDMS composite strain sensors, we comparatively explored the electromechanical properties in the transparent percolated network of solution-processed metallic CNTs by varying an important parameter of the sensor, i.e., the number of sprays of the solution-processed CNTs, which can be used to control and optimize the densities of the metallic CNTs in the CNT−PDMS composite. Our transparent CNT−PDMS composite strain sensors possess high sensitivity, linearity, and stability with a small hysteresis and drifts under controlled fabrication conditions. Finally, to illustrate the applicability of our transparent, flexible strain sensor as epidermal devices, we explored the detections of human activities and emotions by mounting the strain sensors on various spots of skins.

■ RESULTS AND DISCUSSION

A highly purified, solution-processed, and preseparated 99% metallic CNT solution (provided by Nanointegris, Inc.) was used to create the randomly networked CNT transparent film (for details of the metallicity of our CNTs, see the RBM in the Raman spectra in the Supporting Information, Figure S1). The structure of the CNT−PDMS composite strain sensor used in this work is illustrated in Figure 1a. Our CNT−PDMS composite strain sensor was fabricated as a sandwich-like structure by sequentially stacking PDMS layer, metallic CNT film, and PDMS layer. It has been reported that the sandwich-like structured strain sensor could improve the stability during the sensor operations.[1,18,31,42] The fabrication processes of the sensor are as follows: First, the stretchable bottom PDMS layer with a thickness of 0.5 mm was prepared and the surface was then treated by O_2 plasma to make the surface of the PDMS substrate hydrophilic. After that, the surface was functionalized with an amine-terminated group to hold CNTs using a 0.1 g/mL poly-L-lysine solution (purchased from Sigma-Aldrich).[42,43] The substrate was then rinsed with deionized (DI) water. Subsequently, the transparent CNT network film was created by spray-coating of the 99% metallic CNT solution with a concentration of 0.01 mg/mL directly onto the PDMS substrate, followed by thorough rinsing with isopropanol and DI water. An air-spray coating was used as a facile, scalable, and low-cost method[44,45] to deposit solution-processed metallic CNTs. Moreover, to optimize the sensor performance, the density of the CNTs in the network film can easily be controlled by adjusting the number of CNT sprays. As a next step, the CNT film that was deposited on the PDMS substrate was annealed at 90 °C for an hour. Then, two terminals for reading and inducing electrical signals were formed at both ends of CNT percolated network using Ag paste and Cu wire.[42] Finally, an additional top layer of PDMS with a thickness of 0.5 mm was cured on top of the metallic CNT thin film on the top surface of the bottom PDMS layer to form a sandwich-like structure (i.e., three layers stacked by PDMS layer/metallic CNT film/PDMS layer). When the liquid PDMS was casted onto the metallic CNT film, the liquid PDMS penetrated into the interconnected pores of the metallic CNT network. As mentioned above, we used the sandwiched-like strain sensor to reduce the wrinkling and plastic deformation of the networked CNT film that occurs in the case of the CNT film placed on top of the bottom PDMS substrate without an additional PDMS cover layer and therefore could achieve high stability of the sensor.

Our fabricated CNT−PDMS composite strain sensor is clearly flexible and transparent except for the two Ag electrodes. Figure 1b shows an image of the sandwich-structured CNT−PDMS composite strain sensors with great bendability, flexibility, and transparency. It is worthwhile to note that the percolated network film formed by highly purified, solution-processed 99% metallic CNTs in our sensor shows excellent transparency, even with a high density of CNTs in the network film. Note that the optical transparency of the fabricated high-density CNT film (i.e., 150 spray-coats) is greater than 92% in the visible range, as shown in Figure 1c, which is sufficient for an aesthetic view of human applications. Whereas the previously reported strain sensors based on a percolated

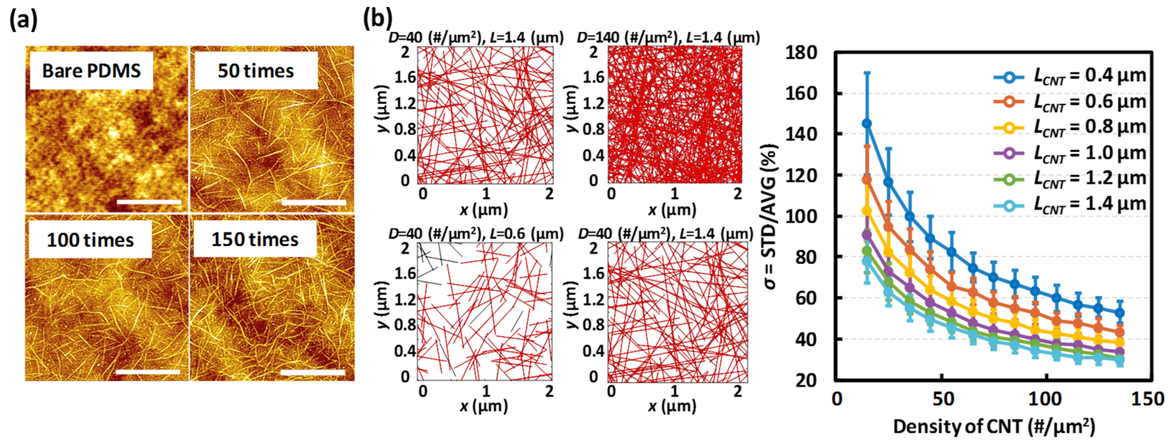

Figure 2. (a) AFM images (2.5 μm × 2.5 μm, z-scale is 10 nm) of the percolated network films of the solution-processed 99% metallic CNTs with different densities. Scale bar is 1 μm. (b) Monte Carlo simulation of the randomly generated CNT network films to evaluate their uniformity. The total length of the CNTs (L_{pixel}) in each pixel of 0.1 μm × 0.1 μm was calculated, and the relative standard deviation (σ) was calculated from the values of L_{pixel} in all pixels. Both higher densities and longer lengths of CNTs improved the uniformity of the film.

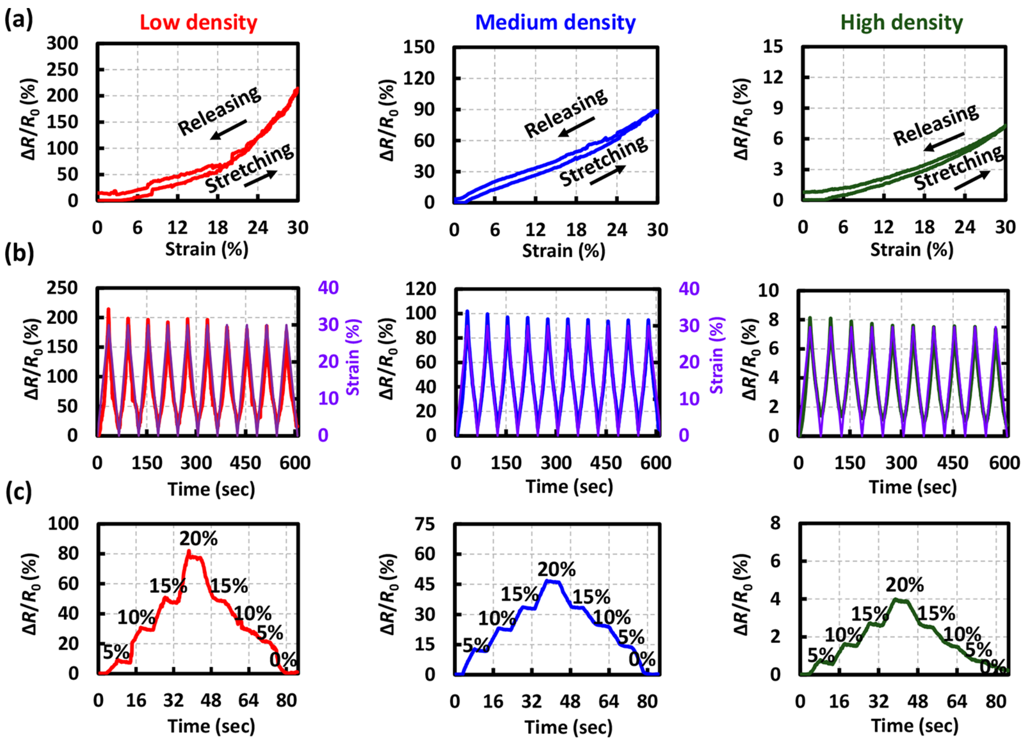

Figure 3. Electromechanical characterization of the CNT−PDMS composite strain sensor with different densities: low, medium, and high density. (a) Piezoresistive responses of the sensors under tensile strains applied from 0% to 30%. (b) Responses of the strain sensors to 10 cycles of stretching/releasing from 0% to 30%. (c) Drift and overshoot performances of the strain sensors with several increasing strains from 0% to 20%.

network of CNTs coupled with elastomer polymers are generally opaque,[27−31] our sensor provided a clear benefit in terms of the excellent transparency with the aid of the highly purified, solution-processed CNTs from the DGU process.[32,40] Therefore, the percolated network by highly purified, preseparated metallic CNTs would be a great candidate[40] for use in strain sensors with both high electrical/mechanical performances and excellent optical transparency.

We explored the morphology of the spray-deposited 99% metallic CNT film on the PDMS substrate with three different densities, as shown in Figure 2a. Images of the CNT networks captured by AFM were found to be highly uniform throughout the samples, which is critical for achieving a uniform performance during sensor operation. The average CNT densities obtained for each number of CNT sprays were extracted as approximately 38 ± 7, 63 ± 6, and 83 ± 5 tubes/μm^2 for 50, 100, and 150 times, respectively. Moreover, we extracted the densities of the CNTs for the three different numbers of spray-coats from scanning electron microscope (SEM) images (for details of SEM images, see Figure S3). Overall, we obtained reliable and similar CNT densities through AFM and SEM evaluations. Note that these CNTs with high metallic purity (99% in our work) were relatively short compared with the CNTs with a low purity because of the greater ultracentrifugation required for higher purity, which results in shorter CNTs; thus, multiple CNT sprays are

DOI: 10.1021/acsami.7b03184
ACS Appl. Mater. Interfaces XXXX, XXX, XXX−XXX

required to form a well-percolated CNT network film.[37−39] Despite the rigorous ultracentrifugation processes, the intensity ratio of the D-band to the G-band in the Raman spectra revealed a lack of any significant structural damage to the high metallic purity CNTs (for details, see Figure S2). Furthermore, it is clear that the standard deviation of the CNT densities in the percolation network decreased as the number of spray-coats increased, which is critical for fabricating sensors with uniform and reliable performance, i.e., for stable sensor operation. Our comprehensive Monte Carlo simulation also confirmed that in the more dense CNTs the variation was reduced, i.e., the uniformity increased, due to an averaging effect, as shown in Figure 2b. Furthermore, it was confirmed that a longer length of CNTs reduced the variation of the film. Therefore, for improved uniformity of the percolated network of a CNT-based strain sensor, high density and long CNTs are both required.

To characterize the electromechanical behaviors of our transparent CNT−PDMS composite strain sensors, they were first fixed to a motorized moving controller (Micro actuator, MA-35). Then, stretching and releasing cycles at different strain levels were applied to the CNT−PDMS composite strain sensor, where the currents were measured under a constant voltage of 5 V using a parameter analyzer (Agilent 4156C). Permanent changes of the CNT−CNT junctions occasionally occurred during the measurement, which demonstrated that the initial resistance values were altered for some of the sensors in the first few stretching and releasing cycles; however, it was observed that the responses of the sensors were highly reproducible. We measured the sensitivity of the sandwich-structured, transparent CNT−PDMS strain sensors with three different number of sprays of the solution-processed CNT solutions, i.e., 50, 100, and 150 times, as shown in Figure 3a. The initial resistance of the strain sensor with the lowest density of CNTs (50 sprays) was relatively large ($R_0 \sim 50$ MΩ) due to the sparse percolation network consisting of fewer CNTs, whereas the strain sensitivity was large, i.e., a 194% relative change in resistance at a 30% strain. This result is most likely due to the fewer parallel conduction pathways that contribute to the electrical conductivity under strain applied to the sensor with a lower density of CNTs.[42] In contrast, when the number of sprays increased to 150 times, the initial resistance clearly reduced down to ($R_0 \sim 5$ MΩ); however, a small sensitivity was obtained, i.e., an 8% relative change in resistance at 30% strain. It was also observed that the sensitivity has a trade-off relationship with the linearity of the sensor. The linearity of our transparent CNT−PDMS composite strain sensor varies depending on the CNT density, which demonstrates that the higher the density of the CNTs is, the better the linearity of the sensors is; i.e., R^2 approaches 0.9639 as the number of sprays increases to 150 times. That is, increasing the density of the CNTs reduces the sensitivity with high linearity. Therefore, the sensitivity and linearity of the sensors can be tuned by simply adjusting the number of CNT sprays based on the individual applications requirements, even accounting for the trade-off relationship. In other words, for low-strain applications, to detect minimal changes in strain, a lower density of CNTs is more appropriate, whereas a higher density of CNTs is better for high-strain applications to detect a wide range of strains (for details of the strain sensitivity and linearity mechanisms in the sensor, see the Monte Carlo simulation in the Supporting Information, Figures S4−S6). It is worth noting that our strain sensor, particularly for the sensor with a medium density of highly purified, solution-processed CNTs, provides acceptable sensitivity and linearity simultaneously in addition to noticeable optical transparency. In addition, we found that a hysteresis was negligible in the sensor response because of the structural robustness originated from a sandwich-like structure.

We also demonstrated the responses of our transparent CNT-PDMS strain sensors under cyclic stretching/releasing in Figure 3b. Overall, relative increases in resistance with increasing applied tensile strains were clearly observed for the CNT−PDMS strain sensors with the three different densities of CNTs. The strain sensors repeated under stretching/releasing of 10 cycles with 0−30% tensile strain. It was observed that the resistance change of the CNT−PDMS composite strain sensor was almost recovered after releasing it from 30% tensile strain. Note that for the sensor with a high density of CNTs, an excellent overlap between $\Delta R/R_0$ and applied strain was obtained; however, for the sensor with a low density of CNTs, there were small differences in the overlap due to the worse linearity, as expected based on Figure 3a.

Another important feature is that the CNT densities in the CNT−PDMS strain sensor significantly affect the sensor reliability or stability. Excellent stability and linearity were achieved with the sensor with a high density of CNTs. The increased density of CNTs resulted in an increased number of junctions between CNTs; in turn, more junctions between CNTs were sustained, even when a high tensile strain was applied, which enhanced the stability of the sensor responses.[42] As a result, excellent stability and recoverability during cyclic stretching/releasing (1000 cycles) were obtained for the sensor with a high density of CNTs without any signal drift or degradation. The baseline resistances in our sensors almost maintained during cyclic tests due to great reliability of the sensors (for details of the long-term stability, see Figure S7).

Furthermore, we investigated the dynamic performances of our transparent CNT−PDMS strain sensors, such as drift and overshoot behaviors, as shown in Figure 3c. The strains ranging from 0% to 20% at 5% intervals were induced to the sensors. Then, the sensors were held at each strain for 5 s.

The strain sensors exhibited small overshoots due to changes in the applied strains in the increasing direction, which is most likely due to the stress relaxation and viscoelastic nature of polymers.[46] Tensile stress develops in the elastomer (i.e., for our case, a PDMS layer) and is then transferred to the CNT−PDMS composite, resulting in the rearrangement and reorientation of the CNTs. This leads to an increase in electrical resistance in the CNT−PDMS strain sensor. However, the tensile stress applied is becoming reduced by a relaxation effect; hence, the arrangement and orientations of the CNTs in the composite are moderately restored within the process time.[46] As a result, the electrical resistance of the sensor gently decreases and essentially reaches to the steady-state value while a constant tensile strain is applied. Note that the measured drift and overshoot performances were more clearly observed for the sensor with a lower density of CNTs, which is closely related to the sensitivity and stability of the sensors as explained.

Our sandwich-structured strain sensors are transparent, stretchable, and sensitive, which allows the fruitful implementation of skin-mountable electronic devices. To evaluate the capability of our strain sensors for detecting human activities and emotions, we explored the performance of the sensors for a wearable, flexible human motion detection platform by simply

DOI: 10.1021/acsami.7b03184
ACS Appl. Mater. Interfaces XXXX, XXX, XXX−XXX

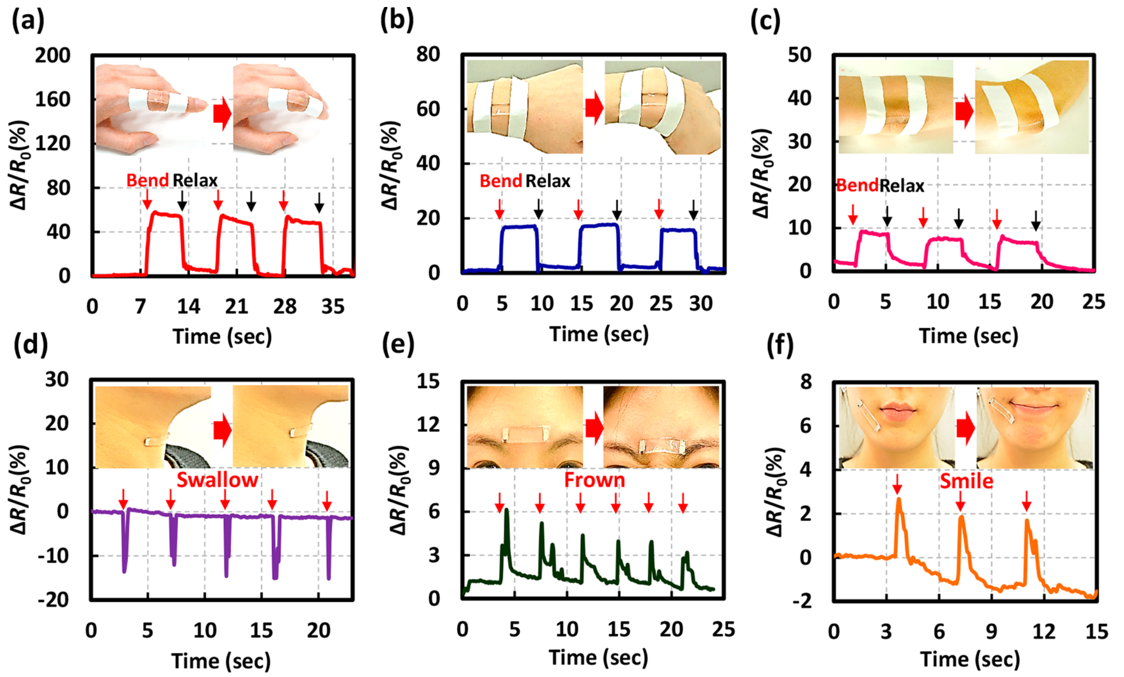

Figure 4. Applications of the transparent CNT−PDMS composite strain sensor to the detections of human activities and emotions: (a) finger joint motion detection, (b) wrist joint detection, (c) elbow joint motion detection, (d) swallowing motion detection on the throat, (e) frowning motion detection on the middle of the forehead, and (f) smiling motion detection on the skin near the mouth.

attaching our transparent CNT−PDMS composite strain sensor with a medium density of CNTs to various locations of the human skins to sense joint motion and detect human emotions. The strain sensor was directly mounted to the skins using an adhesive tape attached to the electrode parts of the strain sensor, as shown in Figure 4. Time-dependent relative changes in resistance of our transparent three-layer stacked CNT−PDMS composite strain sensor were measured by multiple cyclic behaviors of bending/relaxation of the index finger, wrist, and elbow joints, as shown in Figures 4a, 4b, and 4c, respectively. When the joints were bent, the strain sensor accommodated the bending strain, which changed the resistance of the sensor by the applied bending angles. Moreover, when the joints were straightened, the strain induced in the strain sensor relaxed, which demonstrates the recovery of the resistance change to the baseline level. Moreover, we attached our sensors to the throat, middle of the forehead, and skin near the mouth to investigate the ability of the sensor to function as monitoring of swallowing and emotion detectors, as shown in Figures 4d, 4e, and 4f. Interestingly, the $\Delta R/R_0$ responses of the sensor on the throat showed the observed opposite tendency due to the opposite movements of muscles, which is different from the movements of muscles on the middle of the forehead and skin near the mouth. Although we did not additionally measure the sensor array responses to detect a strain distribution on the skin induced by simultaneous movements of multiple muscles, we believe that the distinguishable responses of the sensor on the different spots of skins enable emotion analysis and human−machine interface technology.

CONCLUSIONS

In this paper, we developed a transparent strain sensor with acceptable sensing performances based on solution-processed CNTs and a PDMS composite. In particular, an excellent optical transparency of over 92% was achieved in the visible range due to solution-processed CNT networks, where poorly conducting impurities of unsorted CNTs were eliminated using a DGU process. It was also found that the acceptable sensing performances, such as sensitivity, stability, and linearity, were obtained and controlled by the number of spraying times of the CNTs. Therefore, our results will provide a milestone in the pathway toward human-related applications. Though in this work we used solution-processed metallic CNTs in the sensor, further work is required that investigates solution-processed semiconducting CNTs in a sensor due to their high piezoresistive gauge factors.

EXPERIMENTAL SECTION

Sample Preparation. First, a flexible bottom PDMS substrate was prepared with a thickness of 0.5 mm by a mixture of PDMS prepolymer (Sylgard 184, Dow Corning) and a thermal curing agent in a ratio of 10:1 by weight. After that, the surface of PDMS layer was treated using by O_2 plasma. Then, the surface was functionalized with a 0.1 g/mL poly-L-lysine solution (purchased from Sigma-Aldrich), followed by the substrate rinsed with deionized (DI) water. The CNT network film was readily created by spray-coating (50, 100, and 150 spray-coats) of the 99% metallic CNT solution (provided from Nanointegris, Inc.) with a concentration of 0.01 mg/mL onto the PDMS substrate, followed by rinsing with isopropanol and DI water. As a next step, the deposited CNT on the PDMS substrate was annealed at 90 °C for an hour. For readout of sensor signals, Cu wire was attached at the ends of CNT network film using Ag paste. Finally, a top PDMS layer was casted with the liquid PDMS with a thermal curing agent onto the CNT network film to fabricate a sandwich-like structure.

Sample Characterization. We measure optical transparency of the fabricated CNT−PDMS composite strain sensor using a UV/vis/NIR spectrophotometer (Cary 5000, Agilent). The morphology of CNT film was characterized by AFM (XE-100, Park systems) and SEM (Teneo, FEI). To characterize the electromechanical performances of our transparent CNT−PDMS composite strain sensors, the samples were fixed to a motorized moving stage through a Micro

DOI: 10.1021/acsami.7b03184
ACS Appl. Mater. Interfaces XXXX, XXX, XXX−XXX

actuator (MA-35, Physik Instrumente) while uniform stretching/releasing cycles were induced. The electrical current signal from the sensors were measured using a parameter analyzer (Agilent 4156C) under a constant voltage of 5 V.

■ ASSOCIATED CONTENT

Ⓢ Supporting Information

The Supporting Information is available free of charge on the ACS Publications website at DOI: 10.1021/acsami.7b03184.

More information and details about the metallicity of highly purified, solution-processed 99% metallic carbon nanotube solution through the RBM of the Raman spectra, SEM images of the CNTs deposited on the PDMS substrate, Monte Carlo method-based simulation results, and evaluation of the long-term stability of the CNT−PDMS composited strain sensors (PDF)

■ AUTHOR INFORMATION

Corresponding Authors

*(S.J.C.) E-mail sjchoiee@kookmin.ac.kr.

*(I.P.) E-mail inkyu@kaist.ac.kr.

ORCID

Inkyu Park: 0000-0001-5761-7739

Sung-Jin Choi: 0000-0003-1301-2847

Author Contributions

J.L. and M.L. contributed equally to this work.

Notes

The authors declare no competing financial interest.

■ ACKNOWLEDGMENTS

This work was supported by the National Research Foundation (NRF) of Korea under Grants 2016R1A2B4011366 and 2016R1A5A1012966.

■ REFERENCES

(1) Amjadi, M.; Pichitpajongkit, A.; Lee, S.; Ryu, S.; Park, I. Highly Stretchable and Sensitive Strain Sensor Based on Silver Nanowire−Elastomer Nanocomposite. *ACS Nano* **2014**, *8*, 5154−5163.

(2) Yan, C.; Wang, J.; Kang, W.; Cui, M.; Wang, X.; Foo, C. Y.; Chee, K. J.; Lee, P. S. Highly Stretchable Piezoresistive Graphene-Nanocellulose Nanopaper for Strain Sensors. *Adv. Mater.* **2014**, *26*, 2022−2027.

(3) Hempel, M.; Nezich, D.; Kong, J.; Hofmann, M. A Novel Class of Strain Gauges Based on Layered Percolative Films of 2D Materials. *Nano Lett.* **2012**, *12*, 5714−5718.

(4) Li, X.; Zhang, R.; Yu, W.; Wang, K.; Wei, J.; Wu, D.; Cao, A.; Li, Z.; Cheng, Y.; Zheng, Q.; Ruoff, R. S.; Zhu, H. Stretchable and Highly Sensitive Graphene-on-Polymer Strain Sensors. *Sci. Rep.* **2012**, *2*, 870.

(5) Lu, N. S.; Lu, C.; Yang, S. X.; Rogers, J. A. Highly Sensitive Skin-Mountable Strain Gauges Based Entirely on Elastomers. *Adv. Funct. Mater.* **2012**, *22*, 4044−4050.

(6) Cotton, D. P. J.; Graz, I. M.; Lacour, S. P. A Multifunctional Capacitive Sensor for Stretchable Electronic Skins. *IEEE Sens. J.* **2009**, *9*, 2008−2009.

(7) Sekitani, T.; Nakajima, H.; Maeda, H.; Fukushima, T.; Aida, T.; Hata, K.; Someya, T. Stretchable active-matrix organic light-emitting diode display using printable elastic conductors. *Nat. Mater.* **2009**, *8*, 494−499.

(8) Lipomi, J. D.; Tee, C. B.; Vosgueritchian, M.; Bao, Z. Stretchable Organic Solar Cells. *Adv. Mater.* **2011**, *23*, 1771−1775.

(9) Ko, H. C.; Huang, Y.; Rogers, J. A.; Stoykovich, M. P.; Song, J.; Malyarchuk, V.; Choi, W. M.; Yu, C.-J.; Geddes, J. B., III; Xiao, J.; Wang, S. A. hemispherical electronic eye camera based on compressible silicon optoelectronics. *Nature* **2008**, *454*, 748−753.

(10) Kim, D.-H.; Viventi, J.; Amsden, J. J.; Xiao, J.; Vigeland, L.; Kim, Y.-S.; Blanco, J. A.; Panilaitis, B.; Frechette, E. S.; Contreras, D.; Kaplan, D. L.; Omenetto, F. G.; Huang, Y.; Hwang, K.-C.; Zakin, M. R.; Litt, B.; Rogers, J. A. Dissolvable Films of Silk Fibroin for Ultrathin Conformal Bio-Integrated Electronics. *Nat. Mater.* **2010**, *9*, 511−517.

(11) Kim, R.-H.; Kim, D.-H.; Xiao, J.; Kim, B. H.; Park, S.-I.; Panilaitis, B.; Ghaffari, R.; Yao, J.; Li, M.; Liu, Z.; Malyarchuk, V.; Kim, D.; Le, A.-P.; Nuzzo, R. G.; Kaplan, D. L.; Omenetto, F. G.; Huang, Y.; Kang, Z.; Rogers, J. A. Waterproof AlInGaP Optoelectronics on Stretchable Substrates with Applications in Biomedicine and Robotics. *Nat. Mater.* **2010**, *9*, 929−937.

(12) Kim, D.-H.; Lu, N.; Ma, R.; Kim, Y.-S.; Kim, R.-H.; Wang, S.; Wu, J.; Won, S. M.; Tao, H.; Islam, A.; Yu, K. J.; Kim, T.; Chowdhury, R.; Ying, M.; Xu, L.; Li, M.; Chung, H.-J.; Keum, H.; McCormick, M.; Liu, P.; Zhang, Y.-W.; Omenetto, F. G.; Huang, Y.; Coleman, T.; Rogers, J. A. Epidermal Electronics. *Science* **2011**, *333*, 838−843.

(13) Viventi, J.; Kim, D.-H.; Moss, J. D.; Kim, Y.-S.; Blanco, J. A.; Annetta, N.; Hicks, A.; Xiao, J.; Huang, Y.; Callans, D. J.; Rogers, J. A.; Litt, B. A Conformal, Bio-Interfaced Class of Silicon Electronics for Mapping Cardiac Electrophysiology. *Sci. Transl. Med.* **2010**, *2*, 24ra22.

(14) Pang, C.; Lee, C.; Suh, K.-Y. Recent Advances in Flexible Sensors for Wearable and Implantable Devices. *J. Appl. Polym. Sci.* **2013**, *130*, 1429−1441.

(15) Yamada, T.; Hayamizu, Y.; Yamamoto, Y.; Yomogida, Y.; IzadiNajafabadi, A.; Futaba, D. N.; Hata, K. A stretchable carbon nanotube strain sensor for human-motion detection. *Nat. Nanotechnol.* **2011**, *6*, 296−301.

(16) Amjadi, M.; Kyung, K.-U.; Park, I.; Sitti, M. Stretchable, Skin mountable, and Wearable Strain Sensors and Their Potential Applications: A Review. *Adv. Funct. Mater.* **2016**, *26*, 1678−1698.

(17) Lee, J.; Kim, S.; Lee, J.; Yang, D.; Park, B. C.; Ryu, S.; Park, I. A Stretchable Strain Sensor based on a Metal Nanoparticle Thin Film for Human Motion Detection. *Nanoscale* **2014**, *6*, 11932−11939.

(18) Amjadi, M.; Yoon, Y. J.; Park, I. Ultra-Stretchable and Skin Mountable Strain Sensors using Carbon Nanotubes-Ecoflex Nano-composites. *Nanotechnology* **2015**, *26*, 375501.

(19) Yao, S.; Zhu, Y. Wearable Multifunctional Sensors using Printed Stretchable Conductors made of Silver Nanowires. *Nanoscale* **2014**, *6*, 2345−2352.

(20) Hu, L.; Kim, H. S.; Lee, J. Y.; Peumans, P.; Cui, Y. Scalable Coating and Properties of Transparent, Flexible, Silver Nanowire Electrodes. *ACS Nano* **2010**, *4*, 2955−2963.

(21) Liu, C. H.; Yu, X. Silver nanowire-based transparent, flexible, and conductive thin film. *Nanoscale Res. Lett.* **2011**, *6*, 75.

(22) De, S.; Higgins, T. M.; Lyons, P. E.; Doherty, E. M.; Nirmalraj, P. N.; Blau, W. J.; Boland, J. J.; Coleman, J. N. Silver Nanowire Networks as Flexible, Transparent, Conducting Films: Extremely High DC to Optical Conductivity Ratios. *ACS Nano* **2009**, *3*, 1767−1774.

(23) Lipomi, D. J.; Vosgueritchian, M.; Tee, B. C-K.; Hellstrom, S. L.; Lee, J. A.; Fox, C. H.; Bao, Z. Skin-Like Pressure and Strain Sensors Based on Transparent Elastic Films of Carbon Nanotubes. *Nat. Nanotechnol.* **2011**, *6*, 788−792.

(24) Kang, J. H.; Park, C.; Scholl, J. A.; Brazin, A. H.; Holloway, N. M.; High, J. W.; Lowther, S. E.; Harrison, J. S. Piezoresistive characteristics of single wall carbon nanotube/polyimide nano-composites. *J. Polym. Sci., Part B: Polym. Phys.* **2009**, *47*, 994−1003.

(25) Cai, L.; Song, L.; Luan, P.; Zhang, Q.; Zhang, N.; Gao, Q.; Zhao, D.; Zhang, X.; Tu, M.; Yang, F.; Zhou, W.; Fan, Q.; Luo, J.; Zhou, W.; Ajayan, P. M.; Xie, S. Super-Stretchable, Transparent Carbon Nanotube-Based Capacitive Strain Sensors for Human Motion Detection. *Sci. Rep.* **2013**, *3*, 3048.

(26) Choi, E. S.; Brooks, J. S.; Eaton, D. L.; Al-Haik, M. S.; Hussaini, M. Y.; Garmestani, H.; Li, D.; Dahmen, K. Enhancement of Thermal and Electrical Properties of Carbon Nanotube Polymer Composites by Magnetic Field Processing. *J. Appl. Phys.* **2003**, *94*, 6034−6039.

(27) Hu, N.; Karube, Y.; Arai, M.; Watanabe, T.; Yan, C.; Li, Y.; Liu, Y.; Fukunaga, H. Investigation on Sensitivity of A Polymer/Carbon Nanotube Composite Strain Sensor. *Carbon* **2010**, *48*, 680−687.

(28) Kang, I.; Schulz, M. J.; Kim, J. H.; Shanov, V.; Shi, D. A Carbon Nanotube Strain Sensor for Structural Health Monitoring. *Smart Mater. Struct.* **2006**, *15*, 737−748.
(29) Cohen, D. J.; Mitra, D.; Peterson, K.; Maharbiz, M. M. A Highly Elastic, Capacitive Strain Gauge Based on Percolating Nanotube Networks. *Nano Lett.* **2012**, *12*, 1821−1825.
(30) Song, X.; Liu, S.; Gan, Z.; Lv, Q.; Cao, H.; Yan, H. Controllable fabrication of carbon nanotube-polymer hybrid thin film for strain sensing. *Microelectron. Eng.* **2009**, *86*, 2330−2333.
(31) Roh, E.; Hwang, B.-U.; Kim, D.; Kim, B.-Y.; Lee, N.-E. Stretchable, Transparent, Ultrasensitive, and Patchable Strain Sensor for Human−Machine Interfaces Comprising a Nanohybrid of Carbon Nanotubes and Conductive Elastomers. *ACS Nano* **2015**, *9*, 6252−6261.
(32) Arnold, M. S.; Green, A. A.; Hulvat, J. F.; Stupp, S. I.; Hersam, M. C. Sorting carbon nanotubes by electronic structure using density differentiation. *Nat. Nanotechnol.* **2006**, *1*, 60−65.
(33) Tanaka, T.; Jin, H.; Miyata, Y.; Fujii, S.; Suga, H.; Naitoh, Y.; Minari, T.; Miyadera, T.; Tsukagoshi, K.; Kataura, H. Simple and Scalable Gel-Based Separation of Metallic and Semiconducting Carbon Nanotubes. *Nano Lett.* **2009**, *9*, 1497−1500.
(34) Kim, W.-J.; Usrey, M. L.; Strano, M. S. Selective Functionalization and Free Solution Electrophoresis of Single-Walled Carbon Nanotubes: Separate Enrichment of Metallic and Semiconducting SWNT. *Chem. Mater.* **2007**, *19*, 1571−1576.
(35) Lee, C. W.; Weng, C. H.; Wei, L.; Chen, Y.; Chan-Park, M. B.; Tsai, C. H.; Leou, K. C.; Poa, C. H.; Wang, J.; Li, L. J. Toward High Performance Solution-Processed Carbon Nanotube Network Transistors by Removing Nanotube Bundles. *J. Phys. Chem. C* **2008**, *112*, 12089−12091.
(36) Stokes, P.; Khondaker, S. I. High quality solution processed carbon nanotube transistors assembled by dielectrophoresis. *Appl. Phys. Lett.* **2010**, *96*, 083110.
(37) Wang, C.; Zhang, J.; Ryu, K.; Badmaev, A.; De Arco, L. G.; Zhou, C. Wafer-Scale Fabrication of Separated Carbon Nanotube Thin-Film Transistors for Display Applications. *Nano Lett.* **2009**, *9*, 4285−4291.
(38) Wang, C.; Zhang, J.; Zhou, C. Macroelectronic Integrated Circuits Using High-Performance Separated Carbon Nanotube Thin Film Transistors. *ACS Nano* **2010**, *4*, 7123−7132.
(39) Lee, D.; Seol, M.; Moon, D.; Bennett, P.; Yoder, N.; Humes, J.; Bokor, J.; Choi, Y.-K; Choi, S.-J. High-Performance Thin-Film Transistors Produced from Highly Separated Solution-Processed Carbon Nanotubes. *Appl. Phys. Lett.* **2014**, *104*, 143508.
(40) Green, A. A.; Hersam, M. C. Colored Semitransparent Conductive Coatings Consisting of Monodisperse Metallic Single Walled Carbon Nanotubes. *Nano Lett.* **2008**, *8*, 1417−1422.
(41) Naumov, A. V.; Ghosh, S.; Tsyboulski, D. A.; Bachilo, S. M.; Weisman, R. B. Analyzing Absorption Backgrounds in Single-Walled Carbon Nanotube Spectra. *ACS Nano* **2011**, *5*, 1639−1648.
(42) Lim, M.; Lee, J.; Kim, D. H.; Kim, D. M.; Kim, S.; Choi, S.-J. Comparative Study of Piezoresistance Effect of Semiconducting Carbon Nanotube-Polydimethylsiloxane Nanocomposite Strain Sensor. *IEEE-NANO* **2016**, 755−758.
(43) Wang, C.; Chien, J.-C.; Takei, K.; Takahashi, T.; Nah, J.; Niknejad, A. M.; Javey, A. Extremely Bendable, High-Performance Integrated Circuits Using Semiconducting Carbon Nanotube Networks for Digital, Analog, and Radio-Frequency Applications. *Nano Lett.* **2012**, *12*, 1527−1533.
(44) Vak, D.; Kim, S.-S.; Jo, J.; Oh, S.-H.; Na, S.-I.; Kim, J.; Kim, D.-Y. Fabrication of Organic Bulk Heterojunction Solar Cells by a Spray Deposition Method for Low-cost Power Generation. *Appl. Phys. Lett.* **2007**, *91*, 081102.
(45) Lim, Y.-F.; Lee, S.; Herman, D. J.; Lloyd, M. T.; Anthony, J. E.; Malliaras, G. G. Spray-deposited poly(3,4-ethylenedioxythiophene):poly(styrenesulfonate) top electrode for organic solar cells. *Appl. Phys. Lett.* **2008**, *93*, 193301.
(46) Tobolsky, A. V. Stress relaxation studies of the viscoelastic properties of polymers. *J. Appl. Phys.* **1956**, *27*, 673−685.

DOI: 10.1021/acsami.7b03184
ACS Appl. Mater. Interfaces XXXX, XXX, XXX−XXX